Scripta Materialia 193 (2021) 64–70

Contents lists available at ScienceDirect

Scripta Materialia

journal homepage: www.elsevier.com/locate/scriptamat

Stretching-induced phase transitions in barium titanate-poly(vinylidene fluoride) flexible composite piezoelectric films

Fariha Khan[a], Tim Kowalchik[b], Shad Roundy[b], Roseanne Warren[b,*]

[a] Department of Electrical and Computer Engineering, University of Utah, 50 S. Central Campus Drive, MEB Room 2110, Salt Lake City, UT 84112, United States
[b] Department of Mechanical Engineering, University of Utah, 1495 E 100 S, 1550 MEK, Salt Lake City, UT 84112, United States

ARTICLE INFO

Article history:
Received 13 July 2020
Revised 26 September 2020
Accepted 16 October 2020
Available online 30 October 2020

Keywords:
Piezoelectricity
Polymer matrix composites
Drawing
Phase transformations

ABSTRACT

Improving the piezoelectric performance of poly(vinylidene fluoride) (PVDF) is important for many applications, including energy harvesting. The addition of barium titanate ($BaTiO_3$) nanoparticles in the polymer matrix is a popular method to facilitate β phase formation in PVDF films. For pure PVDF, mechanical drawing (i.e. stretching) has also been shown to increase piezoelectric performance. This work examines, for the first time, the combined effect of stretching and $BaTiO_3$ addition on phase transformations in $BaTiO_3$-PVDF composite films. The results indicate that an alternative phase transformation mechanism occurs during the stretching of PVDF composite films. While stretching of pure PVDF films results in the conversion of non-polar α phase into the electroactive β phase, stretching of $BaTiO_3$-PVDF composite films results primarily in the conversion of weakly electroactive γ phase into the more electroactive β phase. Overall, stretching of $BaTiO_3$-PVDF films is shown to be beneficial for increasing β phase content of PVDF.

Poly(vinylidene fluoride) (PVDF) is a semi-crystalline, polymorph, ferroelectric polymer. It has gained popularity since its discovery as a piezoelectric material in 1961 [1] due to its mechanical flexibility, good dielectric properties, electroactive response, and simple fabrication. While these properties make PVDF a promising material for sensors, actuators, and energy harvesting devices, its low piezoelectric and pyroelectric coefficients compared to pure ceramics limit the use of PVDF in certain applications. Several approaches (e.g., mechanical drawing [2,3], introducing ceramic fillers [4,5], poling at a high electric field [6]) have been tested to enhance PVDF's properties and expand the material's range of application. One promising—but to-date largely untested—approach to increase PVDF β phase content could be a combination of mechanical drawing and ceramic fillers to produce a PVDF-ceramic composite film with improved piezo/pyroelectric response. The goal of this work is to test the effects of varying ceramic filler loading and stretching ratios on the β phase content of barium titanate ($BaTiO_3$)-PVDF thin films.

$BaTiO_3$-PVDF is a widely studied ceramic-polymer ferroelectric composite that is simple to fabricate by a variety of methods [7,8]. $BaTiO_3$ has been shown to increase the β phase content of PVDF polymer matrices when there is a large interaction surface between the polymer and the ceramic particles [2,9]. According to current theory, $BaTiO_3$ particles play a crucial role in the nucleation of PVDF crystal phases and promote the formation of highly electroactive β phases in the polymer chain. The three common PVDF phases, which describe different polymer chain conformations, are α, β, and γ [10]. The non-polar α phase is the most prevalent and can be easily formed in the polymer matrix [1,7,11]. While both β and γ are polar phases, the β phase has a higher dipole moment than the γ phase and yields higher piezoelectric constants [10]. Moreover, $BaTiO_3$ particles help stabilize the β phase of PVDF by reducing the number of defects in the polymer chain [12] and limiting the conversion of the unstable β phase to the otherwise more temperature- and pressure-stable α phase [4].

Previous research indicates that mechanical drawing of PVDF films can also effectively convert non-polar PVDF phases to the β phase [10,13]. The predominant α phase can be converted to the β phase if the drawing temperature is below 100 °C and stretching ratios are on the order of 2–5 [9]. Stretching influences the position of fluorine atoms in the PVDF chain, inducing polymer phase transitions. While both mechanical stretching and the addition of $BaTiO_3$ particles in the PVDF films have independently been shown to improve the β phase content, until now there has been no such investigation of the combined effects of these methods—i.e., the efficacy of stretching $BaTiO_3$-PVDF films as a means to increase PVDF polar phases. In this study, $BaTiO_3$-PVDF thin films of

* Corresponding author.
E-mail address: roseanne.warren@utah.edu (R. Warren).

https://doi.org/10.1016/j.scriptamat.2020.10.036
1359-6462/

0, 5, and 10 wt% $BaTiO_3$ undergo uniaxial mechanical drawing at various stretching ratios until the point of breaking. The effects of the ceramic particles in combination with mechanical drawing are quantified through Fourier transform infrared spectroscopy (FTIR) and X-ray diffraction (XRD) measurements at various stages of fabrication to determine the impact of process parameters on β phase content of PVDF-$BaTiO_3$ composite films.

All materials were purchased from Millipore Sigma and used without modification. PVDF powder (average MW~534,000 g/mol) was dissolved in N, N-dimethylformamide (DMF) at 15 wt% (w/w) in a 45 °C water bath. $BaTiO_3$ nanopowder (cubic crystalline phase, <100 nm particle size, ≥99% trace metals basis) was ground using a mortar and pestle for 5 min to deagglomerate the particles followed by sonication in DMF for 45 min. The homogeneous $BaTiO_3$ dispersion was added to the PVDF-DMF solution at room temperature and sonicated for 1 hour. $BaTiO_3$-PVDF films were made by drop-casting the prepared slurry onto a glass plate using a doctor blade and Kapton tape to obtain uniform film thicknesses. The films were dried at 60 °C in an oven to evaporate the DMF solvent and increase β phase content.

After annealing at 90 °C for 5 h, films were then uniaxially stretched by clamping and hanging weights on a custom-made stretching device. Each film was cut into a 12.7 mm by 38.1 mm sample, which was clamped on its ends between a fixed and a moveable plate, initially without tension. The stretching device and sample were placed into an oven at 80 °C for 1 hour to reach thermal equilibrium. The film was then loaded by placing weights on the moveable end of the device and maintained for 15 min. The deformed film was removed from the oven and allowed to relax. Average elongation was calculated as the ratio of the stretched: unstretched length.

The above procedure was applied to PVDF films with 0, 5, and 10 wt% $BaTiO_3$ content and three different film thicknesses (50, 100, and 150 μm). Scanning electron microscopy (SEM) (FEI Quanta 600F) imaging was used to examine $BaTiO_3$ particle agglomeration and dispersion in the films. Elemental analysis of $BaTiO_3$-PVDF films was conducted using energy-dispersive X-ray spectroscopy (EDX) of carbon-coated films. FTIR spectroscopy (Varian 3100 Excalibur) and XRD (D2 Phaser; 10°–60°; 0.0162°/step sampling rate) were used to measure the β phase content of all films.

Fig. 1a provides a conceptual illustration of the stretching-induced phase transition in $BaTiO_3$-PVDF composite films. In PVDF, the α phase is characterized by an antiparallel TGTG′ conformation of fluorine atoms (T indicating trans arrangement in which the fluorine atoms are oriented at ±180° in the torsional bond arrangement, and G indicating gauche arrangement at ±60°). The γ phase is characterized by TTTGTTTG′ conformation. In contrast, the β phase consists of a TTTT conformation. In pure PVDF films, stretching primarily causes conversion of α phase to β phase, with the antiparallel TGTG′ conformation converting to TTTT conformation and creating dipole moments perpendicular to the polymer chain [1,3]. Fig. 1b provides a SEM image of an unstretched 10 wt% $BaTiO_3$-PVDF film. The $BaTiO_3$ particles are uniformly dispersed, and the film shows minor porosity resulting from the drop-casting method. A SEM image of the same sample, post-stretching (1.1x average elongation) (Fig. 1c), shows lines on the films arising from the uniaxial stretching as well as microtears along $BaTiO_3$ particles. EDX measurements of carbon-coated samples confirm the expected doubling of Ba and Ti atomic content for 5 and 10 wt% $BaTiO_3$-PVDF films (Fig. 1d).

Fig. 2 characterizes the force required to stretch the $BaTiO_3$-PVDF films, and the resulting elongation. Data points in Fig. 2 represent average values of two samples of each film; in all cases, the results differed by <10% between samples. In addition, elongation values in Fig. 2 represent average values for the full length of the stretched film; localized film stresses and stretching ratios likely vary across the films and may be higher in areas of the sample closer to the breaking line. This is especially true for 5 and 10 wt% $BaTiO_3$ films, which did not stretch as uniformly as pure PVDF.

The maximum load applied to the films at their breaking point is an important indication of our ability to mechanically stretch the composite films using a uniaxial stretching setup. The load at breaking increases with film thickness for all values of $BaTiO_3$ wt% (Fig. 2a). Pure PVDF shows the highest increase in strength as thickness increases from 50 μm to 150 μm, compared to only a slight increase for the composite films. The observed tendency of $BaTiO_3$-PVDF composite films to rip easily during stretching, even at higher thicknesses, is likely due to stress concentrations created by the introduction of $BaTiO_3$ particles. The introduction of filler particles creates micro-tears in the film during stretching, visible in Fig. 1c; we suspect that subsequent large-scale tears propagating from these micro-tears are the primary failure mechanism for the composite films.

For all film thicknesses, increasing $BaTiO_3$ wt% results in decreasing achievable stretching ratios for composite films undergoing uniaxial stretching (Fig. 2b). As expected, the pure PVDF film shows the most substantial elongation (1.5x for the 150 μm film). At 5 wt% $BaTiO_3$, a stretching ratio approaching 1.5x is achieved with 150 μm film thickness; at 10 wt% $BaTiO_3$, all films failed with less than 1.2x elongation. While pure PVDF films were observed to easily deform along their entire length during stretching, the composite films deformed in localized regions mid-length before sudden tearing. Variations in localized elongation, along with sample-to-sample differences, may account for the unexpected result observed for 10 wt% $BaTiO_3$, where the 100 μm film produced higher elongation than the 150 μm film. With the significant decrease in maximum elongation observed when $BaTiO_3$ content increases from 5 to 10 wt%, we conclude that $BaTiO_3$ content in $BaTiO_3$-PVDF thin films should be limited to 5% if mechanical stretching is to be performed.

To evaluate and compare the changing β phase content of 0, 5, and 10 wt% $BaTiO_3$-PVDF films, FTIR and XRD are used in conjunction. For FTIR spectra, the primary peak of α phase is 763 cm^{-1}, with additional α phase peaks located at 408, 532, 795, 854, 975, and 1209 cm^{-1} [7,10,13–15]. Unique β phase peaks are located at 445, 464, 1276, and 1431 cm^{-1}; unique γ phase peaks are located at 812 and 1234 cm^{-1}. The peak at 840 cm^{-1} is characteristic of both β and γ phases [8].

For pure PVDF (0 wt% $BaTiO_3$, **Fig. 3a**), the unannealed film is predominantly α phase, missing significant peaks from both β and γ phases. There is a small increase in the γ peak at 812 cm^{-1} with annealing, followed by increases in β phase peaks (and corresponding reductions in α and γ phase peaks) with stretching. Specifically, the stretched PVDF film shows strong peaks at 445, 464, 840, 1276, and 1431 cm^{-1}. While the 840 cm^{-1} peak is representative of both β and γ, the reduction in γ phase peak at 812 cm^{-1} indicates the gains at 840 cm^{-1} are likely predominantly β phase. This result is consistent with literature reports of pure PVDF film stretching [10,16–18].

There is a considerable improvement in β phase content with the introduction of $BaTiO_3$ in PVDF, with unstretched 5 and 10 wt% $BaTiO_3$-PVDF films (Fig. 3b and c, respectively) showing higher β phase peaks (445, 464, 840, 1431 cm^{-1}) compared to pure, unstretched PVDF. The stretched $BaTiO_3$-PVDF composite films show strong peaks at 445, 464, 840, 1276, and 1431 cm^{-1}. Similar to the pure PVDF film, there is a noticeable decrease in γ phase peaks at 812 and 1234 cm^{-1} with stretching, suggesting conversion of γ phase to β phase when $BaTiO_3$-PVDF films are stretched. Note that as 0, 5, and 10 wt% $BaTiO_3$ films are stretched, decreasing film thickness results in an overall reduction in FTIR absorbance;

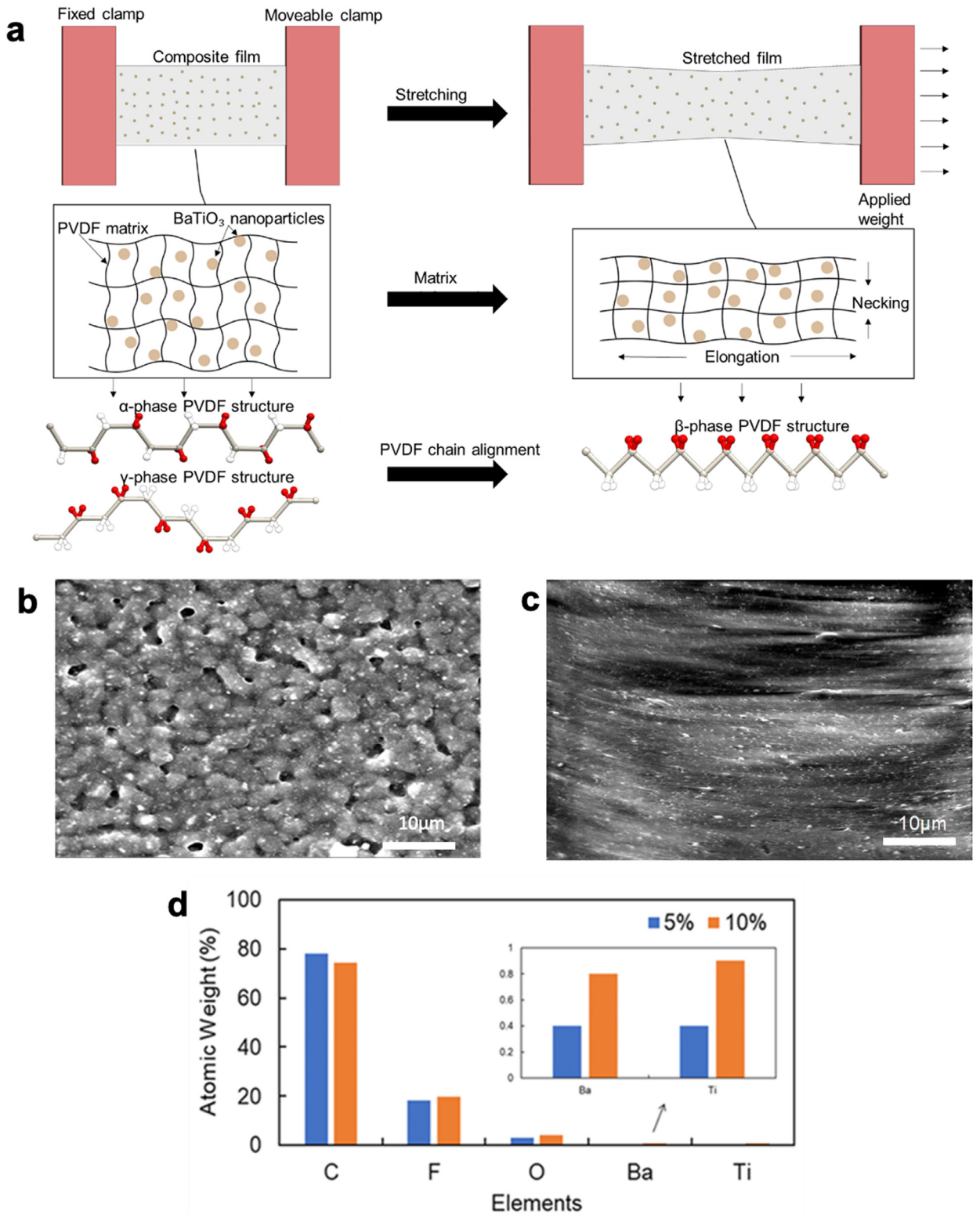

Fig. 1. a) Conceptual illustration of $BaTiO_3$-PVDF composite structure before and after stretching, including the applied uniaxial stretching mechanism, polymer matrix elongation, and conversion of α and γ phase PVDF to β phase. SEM images of a $BaTiO_3$-PVDF composite film (10 wt%) before (b) and after (c) stretching. d) EDX measurements of 5 and 10 wt% $BaTiO_3$ -PVDF films.

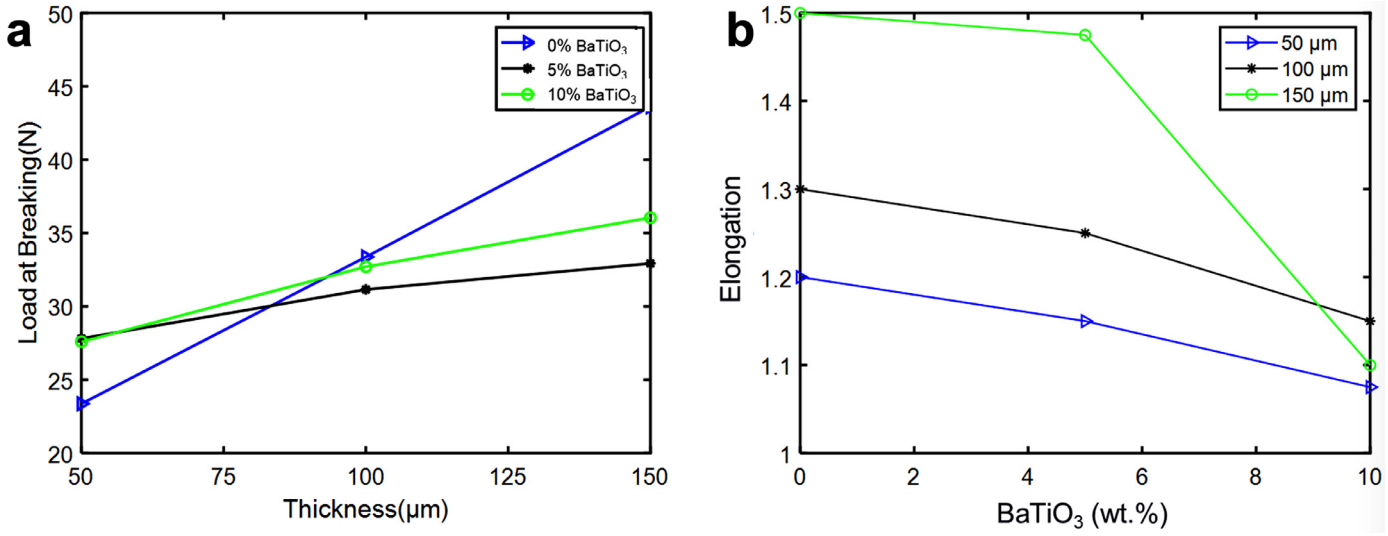

Fig. 2. Effect of starting film thickness and $BaTiO_3$ wt% on the maximum load applied to the $BaTiO_3$-PVDF films at breaking (a) and the maximum elongation (stretching ratio) at breaking (b).

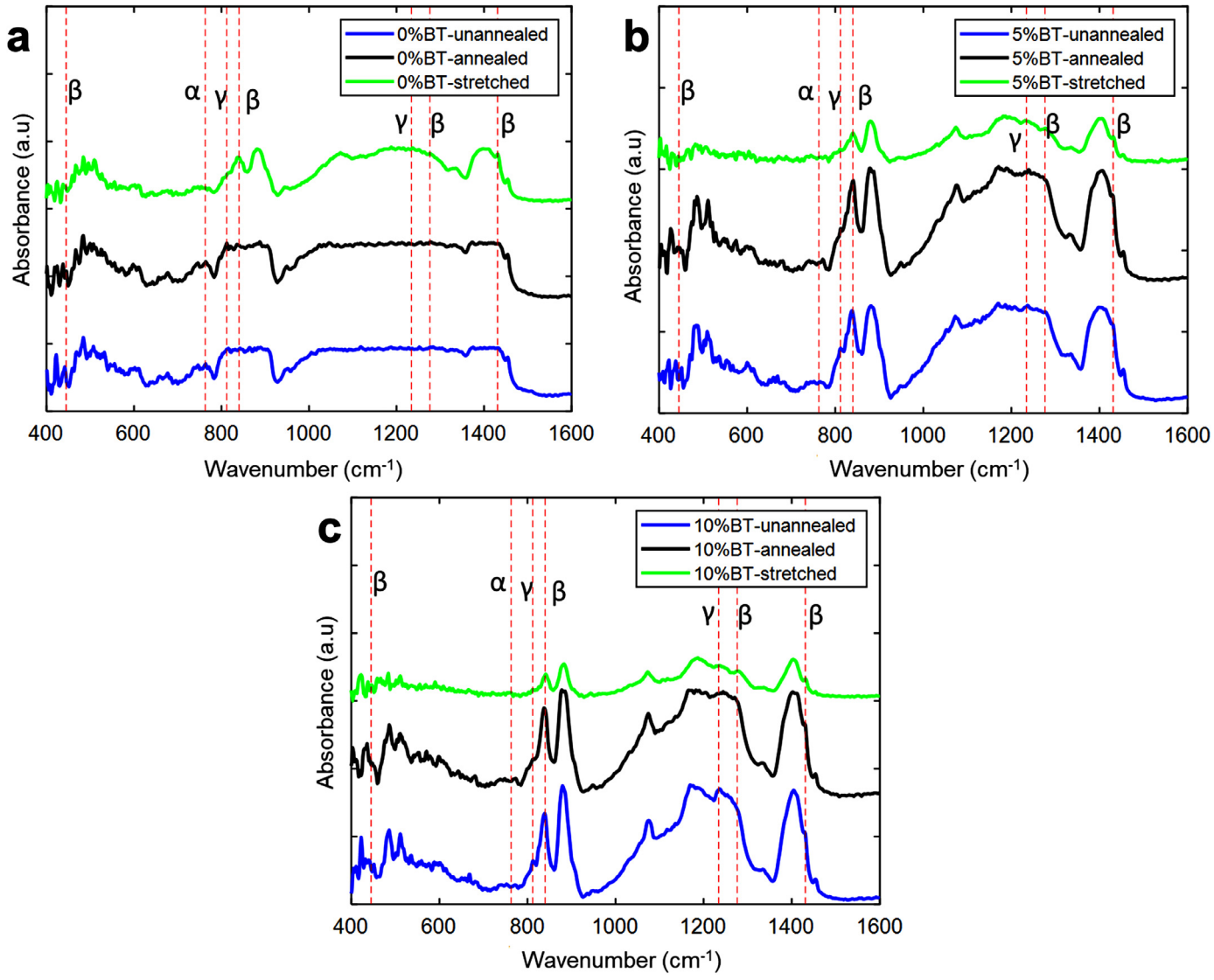

Fig. 3. FTIR spectrum of unannealed, annealed and stretched $BaTiO_3$-PVDF films with: a) 0 wt% $BaTiO_3$ (BT) (pure PVDF), (b) 5 wt% $BaTiO_3$-PVDF, (c) 10 wt% $BaTiO_3$-PVDF.

Table 1
Quantitative comparison of electroactive phase content.

$BaTiO_3$ content	Sample	F($\beta+\gamma$)
0	Unannealed	52.9%
wt%	Annealed	52.4%
	Stretched	67.7%
5	Unannealed	71.7%
wt%	Annealed	75.2%
	Stretched	70.2%
10	Unannealed	79.8%
wt%	Annealed	76.2%
	Stretched	79.8%

therefore, quantitative comparisons of peak heights are needed to more rigorously evaluate changes in phase content with film stretching.

To quantitatively evaluate the electroactive ($\beta+\gamma$) phase fraction, we apply the equation proposed by Gregorio et al. [7] to the FTIR results of Fig. 3:

$$F(\beta+\gamma)=\frac{A_{\beta+\gamma}}{A_{\beta+\gamma}+1.26A_{\alpha}} \quad (1)$$

where A_α and $A_{\beta+\gamma}$ are the absorption bands at 763 cm^{-1} and 840 cm^{-1}, respectively, and the factor 1.26 represents the absorption coefficient ratio of β and α phases ($\frac{K_\beta}{K_\alpha}$)(**Table 1**). We note that Eq. (1) can be used for pure β phase quantification only when γ phase content can be assumed negligible [19]; Fig. 2 results clearly indicate the presence of γ phase in the pure PVDF and $BaTiO_3$-PVDF films, making this a combined $\beta+\gamma$ phase content estimate. For unannealed and unstretched films, the results indicate a substantial increase in electroactive phases when the $BaTiO_3$ fraction increases from 0 to 5 wt% ($\beta+\gamma$ content increases from 53% to 72%), followed by a smaller increase in electroactive phases when the $BaTiO_3$ fraction increases from 5 to 10 wt% ($\beta+\gamma$ content increases from 72% to 80%). The effectiveness of increasing $BaTiO_3$ content in promoting $\beta+\gamma$ phases likely reduces at higher wt% due to the agglomerating tendency of $BaTiO_3$ nanoparticles producing proportionally less electroactive phase nucleation per filler particle. Annealing does not appear to have a large impact, with all films remaining at approximately the same $\beta+\gamma$ phase content before and after annealing (< 4% change). Stretching results in a significant increase in total electroactive phases for pure PVDF but produces a negligible change in the 5 and 10 wt% composite films. For both 5 and 10 wt% $BaTiO_3$ films, combined electroactive phase content is approximately the same for unannealed vs. stretched films (within 1.5%). We note that separate quantification of β and γ phases using the peak-to-valley method proposed by Cai et al. [16] is complicated here by the presence of $BaTiO_3$ particles in the composite films, as $BaTiO_3$ FTIR peaks overlap with those required for peak-to-valley quantification in PVDF. This issue is further explained in the Supplementary Material (Table S1, Fig. S4), including close-up views of β and γ phase peaks at 812 cm^{-1} (Fig. S1), 445 cm^{-1} and 464 cm^{-1} (Fig. S2), as well as 1234 cm^{-1} and 1276 cm^{-1} (Fig. S3).

XRD measurements of annealed and stretched films (0, 5, 10 wt% $BaTiO_3$) (**Fig. 4**) are used to validate FTIR observations, and to further distinguish between β vs. γ phase transitions occurring in the films. For PVDF, α phase peaks occur at 2θ values of 17.6°, 18.3°, 19.8°, and 26.5°; β phase peaks occur at 20.3°, 20.4°, and 20.6°; and γ phase peaks occur at 18.5°, 19.2° and 20.0° [16,20–23]. $BaTiO_3$ peaks occur at 2θ values of 22.2°, 31.5°, 38.9°, 45.0°, 50.8°, and 56.0° [24,25].

Fig. 4a, b compares XRD measurements for annealed and stretched films, respectively, for different $BaTiO_3$ wt%. For 5 and 10 wt% films, $BaTiO_3$ peaks are visible as expected. In all cases, the primary β phase peak appears larger in the stretched films, with higher $BaTiO_3$ content generally corresponding to a higher β phase peak value among the samples. A comparison of annealed vs. stretched films shows an increase in β phase peaks with stretching, and the reduction of a "shoulder" of α and γ phase content in the 17.5°- 20.0° region (Fig. 4a, b). For pure PVDF specifically, we note a decrease in α phase peaks at 17.6°, 18.3°, and 26.5° with stretching, along with a decrease in the γ phase peak at 19.2° and an increase in β phase peaks at 20.3° and 20.6° (Fig. 4c). The 5 wt% $BaTiO_3$ film shows a similar result, with a slight decrease in α phase peaks at 17.6°, 18.3° and a large decrease in the α phase peak at 19.8°. The 5 wt% $BaTiO_3$ film also shows a decrease in the γ phase peaks at 18.5° and 19.2°, and an increase in β phase peaks at 20.3°, 20.4°, and 20.6° (Fig. 4d). The 10 wt% $BaTiO_3$ film shows decreased α phase peaks at 17.6°, 19.8°, and 26.5°; decreased γ phase peaks at 18.5°, 19.2° and 20.0°; and increased β phase peaks at 20.3°, 20.4°, and 20.6° (Fig. 4e). These results suggest increased β phase content with loss of α and γ phase content in every stretched film.

Comparison of FTIR and XRD results suggests that stretching of $BaTiO_3$-PVDF films results primarily in the conversion of γ to β phase, while stretching of pure PVDF films results primarily in the conversion of α to β phase. While quantitative FTIR results in Table 1 indicate a negligible change in $\beta+\gamma$ phase with stretching of $BaTiO_3$-PVDF films, a study of individual β and γ phase peaks in FTIR and XRD measurements clearly indicates an increase in β phase content and a decrease in γ phase content. Specifically, FTIR results for 5 and 10 wt% $BaTiO_3$-PVDF films show the development of unique β phase peaks at 1276 and 1431 cm^{-1} and a decrease in unique γ phase peaks at 812 and 833 cm^{-1} with stretching. These changes leave the 840 cm^{-1} combined $\beta+\gamma$ phase peak relatively stable, with the β phase gains balancing the γ phase decrease. There are several probable explanations for the observed difference in predominant phase conversion mechanisms for pure PVDF vs. $BaTiO_3$-PVDF films with stretching. Pure PVDF films have a higher percentage of α phase in their pre-stretched form compared to $BaTiO_3$-PVDF; it is possible that the low α phase content of the composite films does not effectively convert to β phase with stretching (previous studies of pure PVDF stretching typically report ~20% residual α phase with 4–5x elongation [13,26]). Another possibility is that organic-inorganic interactions between the $BaTiO_3$ filler and the polymer decreases the mobility of the polymer chain [1,7], such that higher elongation ratios would be needed for α to β phase conversion in $BaTiO_3$-PVDF composites.

In conclusion, the results presented here indicate a promising shift of PVDF α and γ phases to β phase upon stretching of $BaTiO_3$-PVDF composite films. The maximum electroactive phase content reached in the stretched composite films is 80%, compared to 68% in stretched PVDF. While increasing $BaTiO_3$ content from 5 to 10 wt% results in higher β phase content, the 10 wt% films have significantly lower mechanical elasticity and break at lower elongation ratios. Mechanical stretching of the composite films is also observed to be less uniform than pure PVDF films. XRD and the FTIR results indicate that PVDF β phase is dominant in the stretched composite films, as stretching predominantly converts γ phase content to β phase in the composite films. In future work, we suggest the tradeoff between increased electroactive response and lower mechanical flexibility in $BaTiO_3$-PVDF composite films may be improved with surface modification of the $BaTiO_3$ nanoparticles. Surface modification reduces $BaTiO_3$ particle agglomeration and creates stronger interfacial bonding between $BaTiO_3$ and PVDF [27]. We hypothesize these effects will improve the mechanical properties $BaTiO_3$-PVDF composite films, enabling larger elongation ratios than achieved in this work and potentially greater conversion of α and γ phase to β phase.

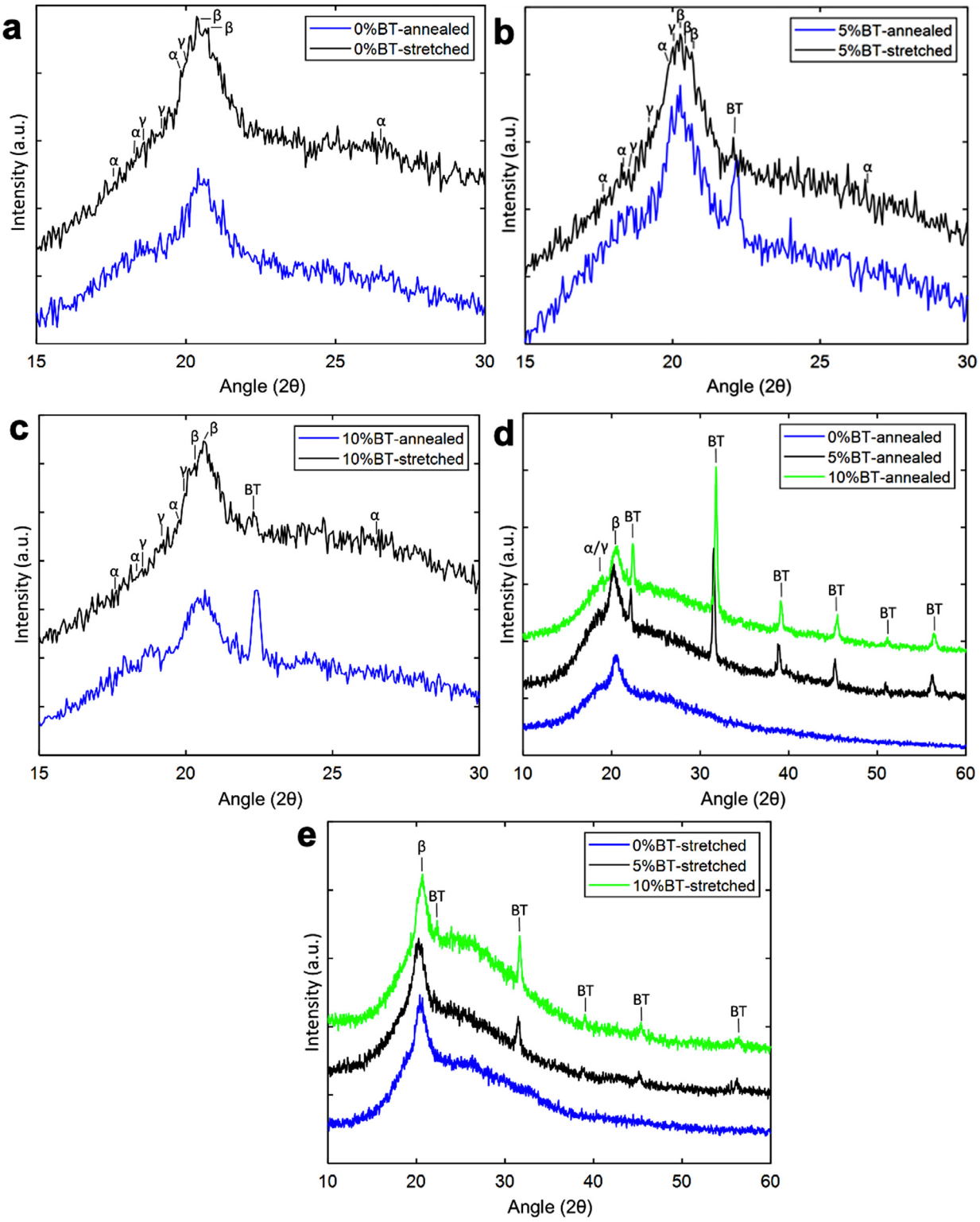

Fig. 4. Comparison of XRD results for a) annealed PVDF films with 0, 5, and 10 wt% $BaTiO_3$, b) stretched PVDF films with 0, 5, and 10 wt% $BaTiO_3$, c) pure PVDF annealed and stretched films, d) 5 wt% $BaTiO_3$-PVDF annealed and stretched films, and e) 10 wt% $BaTiO_3$-PVDF annealed and stretched films.

Declaration of Competing Interest

The authors declare that they have no known competing financial interests or personal relationships that could have appeared to influence the work reported in this paper.

Acknowledgments

This work is supported by National Science Foundation of United States (Award No. 1936636). The authors are grateful to the staff of the University of Utah Nanofab, Surface Analysis Lab, and Materials Characterization Lab for their assistance.

Supplementary materials

Supplementary material associated with this article can be found, in the online version, at doi:10.1016/j.scriptamat.2020.10.036.

References

[1] Y. Bormashenko, R. Pogreb, O. Stanevsky, E. Bormashenko, Polym. Test. 23 (2004) 791–796.
[2] A. Ferri, S. Barrau, R. Bourez, A. Da Costa, M.H. Chambrier, A. Marin, J. Defebvin, J.M. Lefebvre, R. Desfeux, Compos. Sci. Technol. 186 (2020) 107914.
[3] L. Li, M. Zhang, M. Rong, W. Ruan, RSC Adv. 4 (2014) 3938–3943.
[4] A.D. Hussein, R.S. Sabry, O.A.A. Dakhil, R. Bagherzadeh, J. Phys.: Conf. Ser. 1294 (2019) 022012.
[5] A. Baji, Y.W. Mai, in: T. Lin (Ed.), Novel Aspects of Nanofibers, IntechOpen, United Kingdom, 2018, pp. 137–149.
[6] A. Hartono, Darwin, S. Ramli, Satira, M. Djamal, Herman, AIP Conf. Proc. 1719 (2016) 030021.
[7] R. Gregorio, M. Cestari, F.E. Bernardino, J. Mater. Sci. 31 (1996) 2925–2930.
[8] A.A. Rodríguez-Rodríguez, N.A. Morales-Carrillo, C. Gallardo-Vega, G.F. Hurtado-López, J.A. Cepeda-Garza, V. Corral-Flores, Mater. Res. Soc. Symp. Proc. 1479 (2012) 33–38.
[9] R. Gregorio, E.M. Ueno, J. Mater. Sci. 34 (1999) 4489–4500.
[10] P. Martins, A.C. Lopes, S. Lanceros-Mendez, Prog. Polym. Sci. 39 (2014) 683–706.
[11] Z. Yin, B. Tian, Q. Zhu, C. Duan, Polymers (Basel) 11 (2019) 2033.
[12] M. Sharma, J.K. Quamara, A. Gaur, J. Mater. Sci. Mater. Electron 29 (2018) 10875–10884.
[13] A. Salimi, A.A. Yousefi, Polym. Test. 22 (2003) 699–704.
[14] S.H. Lee, H.H. Cho, Fibers Polym. 11 (2010) 1146–1151.
[15] M. Khalifa, S. Janakiraman, S. Ghosh, A. Venimadhav, S. Anandhan, Polym. Compos. 40 (2019) 2320–2334.
[16] X. Cai, T. Lei, D. Sun, L. Lin, RSC Adv. 7 (2017) 15382–15389.
[17] M. Benz, W.B. Euler, O.J. Gregory, Macromolecules 35 (2002) 2682–2688.
[18] S.K. Karan, D. Mandal, B.B. Khatua, Nanoscale 7 (2015) 10655–10666.
[19] S.F. Mendes, C.M. Costa, C. Caparros, V. Sencadas, S. Lanceros-Méndez, J. Mater. Sci. 47 (2012) 1378–1388.
[20] H. Bai, X. Wang, Y. Zhou, L. Zhang, Prog. Nat. Sci. Mater. Int. 22 (2012) 250–257.
[21] T. Nishiyama, T. Sumihara, E. Sato, H. Horibe, Polym. J. 49 (2017) 319–325.
[22] L. Ruan, X. Yao, Y. Chang, L. Zhou, G. Qin, X. Zhang, Polymers (Basel) 10 (2018) 1–27.
[23] I.Y. Abdullah, M.H.H. Jumali, M. Yahaya, H.M. Shanshool, Adv. Environ. Biol. 9 (2015) 20–27.
[24] N.M. Zali, C.S. Mahmood, S.M. Mohamad, C.T. Foo, J.A. Murshidi, AIP Conf. Proc. 1584 (2014) 160–163.
[25] Z. Lazarević, N. Romčević, M. Vijatović, N. Paunović, M. Romčević, B. Stojanović, Z. Dohčević-Mitrović, Acta Phys. Pol. A 115 (2009) 808–810.
[26] V. Sencadas, R. Gregorio, S. Lanceros-Méndez, J. Macromol. Sci. Part B Phys. 48 (2009) 514–525.
[27] K. Yu, H. Wang, Y. Zhou, Y. Bai, Y. Niu, J. Appl. Phys. 113 (2013) 034105.